

## PAPER

[View Article Online](#)  
[View Journal](#) | [View Issue](#)Cite this: *J. Mater. Chem. C*, 2025,  
13, 10804Highly transient and recyclable MoS<sub>2</sub>/PVA  
pressure sensor for sustainable healthcare  
and consumer electronic applications†Naveen Bokka, <sup>a</sup> Nongthombam Joychandra Singh, <sup>b</sup>  
Chandra Sekhar Reddy Kolli <sup>b</sup> and Parikshit Sahatiya <sup>\*bc</sup>

The advent of electronic gadgets has brought convenience to daily life; however, it has also contributed to the proliferation of electronic sensors, exacerbating the issue of electronic waste (e-waste). Previous efforts toward transient electronics aimed at addressing e-waste have faced challenges due to material wastage. To overcome these limitations, it would be beneficial to develop a process wherein transient electronics are reusable. In this study, a transient pressure sensor was fabricated using MoS<sub>2</sub> and PVA, and its degradation in an aqueous medium was subsequently demonstrated. The MoS<sub>2</sub>, which served as the active material, was recovered after degradation and reused for the fabrication of another pressure sensor. Electrical tests on the sensor demonstrated its piezoresistive nature, with the device capable of detecting various pressures in the range of 1–3 kPa, exhibiting a sensitivity of 0.87 kPa<sup>−1</sup>. A cyclic test was also conducted for 1200 cycles, revealing excellent durability. Moreover, the sensor maintained stable performance over three months without any loss in electrical properties. The fabricated sensor was employed in real-time applications, such as detecting the radial artery pulse (hand), carotid artery pulse (neck), and varying air pressures from a syringe bulb, and it was also used as directional keys for a gaming console. The MoS<sub>2</sub>/PVA sensor dissolved completely within 300 s. The performance of the recycled MoS<sub>2</sub>/PVA sensor was compared with that of the original MoS<sub>2</sub>/PVA sensor, showing negligible differences. The successful demonstration of a MoS<sub>2</sub>/PVA-based transient and recyclable pressure sensor holds immense potential for future IoT applications.

Received 10th January 2025,  
Accepted 15th April 2025

DOI: 10.1039/d5tc00117j

[rsc.li/materials-c](https://rsc.li/materials-c)

## Introduction

Every year, technology undergoes rapid advancements, deeply influencing various aspects of modern societal lifestyles.<sup>1</sup> The increasing reliance on electronics contributes to an enhanced quality of life and improvements in human health.<sup>2</sup> Advances in processing techniques have led to enhanced electronic performance, driving consumers to purchase more electronic products and discard older ones (*e.g.*, smartwatches and smartphones). These discarded electronics become electronic waste (e-waste).<sup>3</sup> E-Waste presents a hazardous threat to the environment, posing risks to the health of living beings.<sup>3</sup> According to

surveys, e-waste production has escalated to a concerning rate of 7.5 kg per person per year.<sup>1,4</sup> Only a fraction, approximately 10–20%, of this waste is recycled, while the majority is disposed of in landfills.<sup>5</sup> This waste releases hazardous chemicals and toxic materials into the environment.<sup>3</sup> According to the World Economic Forum, global electronic waste production surpassed 53.6 million tons in 2019, with projections indicating it could reach 74.7 million tons by 2030.<sup>6,7</sup> Recently, a new type of technology has emerged, completely opposite to conventional electronics, known as transient electronics.<sup>8,9</sup> These electronics are designed to dissolve or disintegrate after use, thereby minimizing e-waste.<sup>10</sup> However, current applications are largely limited to therapeutics and biologically integrated circuits, which are often made from silicon-based materials that themselves contribute to e-waste.<sup>3,11</sup> The aim is to develop fully recyclable electronics, in which environmentally harmful materials are reclaimed and reused.

In recent years, research communities have increasingly focused on this issue. A recent report highlighted the progress in recyclable electronics. Xu *et al.* developed a recyclable ink composed of polyvinyl alcohol and a liquid metal. Flexible sensors

<sup>a</sup> Department of Electronics and Communication Engineering, B V Raju Institute of Technology, Narsapur, Medak 502313, India<sup>b</sup> Department of Electrical and Electronics Engineering, Birla Institute of Technology and Science Pilani, Hyderabad Campus, Hyderabad 500078, India.E-mail: [parikshit@hyderabad.bits-pilani.ac.in](mailto:parikshit@hyderabad.bits-pilani.ac.in)<sup>c</sup> Materials Center for Sustainable Energy and Environment, Birla Institute of Technology and Science Pilani, Hyderabad Campus, Hyderabad-500078, India† Electronic supplementary information (ESI) available. See DOI: <https://doi.org/10.1039/d5tc00117j>

fabricated using this liquid metal ink offer a wide range of applications, high sensitivity, and consistently stable signal generation. Additionally, the liquid metals in these printed flexible sensors can be recycled under alkaline conditions.<sup>12</sup> Williams *et al.*<sup>13</sup> fabricated transistors by utilising carbon nanotube as a semiconductor, nanocellulose as a dielectric, graphene as a conductor, and paper substrate. These transistors demonstrate consistent performance up to six months in ambient conditions. Later, decomposed carbon nanotubes and graphene inks can be recollected for recycling and reprinting of new transistors.<sup>13</sup> In another study, Liu *et al.*<sup>14</sup> reported on the recycling of silver nanowire (AgNW) percolation networks to enable soft electronics. The AgNW network film can be recycled multiple times, with no significant changes in morphology or performance degradation. Additionally, a transient sensor patch has been fabricated using AgNW electrodes and a water-soluble polymer substrate, and completely recycled.<sup>14</sup> Guo *et al.*<sup>15</sup> presented a conductive recyclable composite for wearable electronics, including a capacitive pressure sensor, a triboelectric nanogenerator, and a flexible keyboard. This composite material is recyclable and degradable. Combining multiple functions and sustainable manufacturing in one electronic device is highly desirable for design and fabrication.<sup>15</sup> Tengyang *et al.*<sup>16</sup> presented a recyclable dual-mode thin-film device capable of simultaneously performing light emission and heat management. The device demonstrates complete recyclability and a reconstruction ability, maintaining performance integrity even after multiple recycling cycles. Soft-matter electronics with characteristics including resilience, repairability, and recyclability can reach the same level of advancements as industrial electronics.<sup>16</sup> Tavakoli *et al.*<sup>17</sup> reported novel microchip-integrated soft-matter electronics with the recycling of advanced skin patches with embedded electrodes, microchips antennas, and sensors, capturing human electrophysiological signals.<sup>17</sup>

The unique properties of two-dimensional (2D) materials have attracted significant attention within the scientific community. 2D materials have exceptional electrical, electronic, mechanical, and optoelectronic properties and offer a promising avenue for enhancing the performance of electronic devices.<sup>18,19</sup> After, graphene, a diverse range of 2D materials offer exceptional electrical, mechanical, and optoelectronic characteristics, particularly 2D transition-metal dichalcogenides (TMDs) like molybdenum disulfide ( $\text{MoS}_2$ ), making them ideal candidates for applications in transistors, photodetectors, flexible electronics, and more.<sup>20</sup> Despite these advantages, the insolubility of pristine 2D  $\text{MoS}_2$  poses challenges for their use in transient electronics, which require materials that can dissolve or degrade in a controlled manner.<sup>21</sup> The processing and integration of 2D TMDs into transient devices can be complex and costly.<sup>22</sup> Nevertheless, this challenge can be turned into an opportunity by focusing on the recyclability of these materials. Since pristine 2D  $\text{MoS}_2$  is insoluble in water, devices made from these materials can be recovered after use, allowing the valuable material to be recycled and reused. This approach addresses the environmental concerns associated with electronic waste and enhances the sustainability and

economic viability of transient electronic devices by promoting the recycling of key materials.

This work presents a recyclable and reusable pressure sensor by utilizing 2D  $\text{MoS}_2$  as the functional material and water-soluble polyvinyl alcohol (PVA) polymer. The benefits of PVA polymer are its biocompatibility, flexibility, durability, water solubility, and low cost, making it suitable for a recyclable pressure sensor. Notably, the plain PVA film exhibits very high resistance ( $\sim 5.4 \text{ G}\Omega$ ),<sup>8</sup> with the conductivity of the fabricated device solely attributed to 2D  $\text{MoS}_2$ . Sensor fabrication process commences with the synthesis of 2D  $\text{MoS}_2$  material *via* the hydrothermal method, followed by comprehensive characterization of  $\text{MoS}_2$ . Subsequently, the synthesized  $\text{MoS}_2$  liquid is blended with PVA polymer to form a film. The sensor exhibits a piezoresistive nature and was tested across various pressures, demonstrating its capability to detect pressures within 1–3 kPa, with sensitivity of  $0.87 \text{ kPa}^{-1}$ . Additionally, the sensor demonstrates good durability of up to 1200 cycles, rise and fall time of 260 ms and 320 ms, respectively. Furthermore, the recyclable  $\text{MoS}_2$ /PVA pressure sensor was utilized for detecting radial artery pulse (hand), carotid artery pulse (neck), different air pressures from syringe bulb, and also serves as a directional key for the gaming console. Polyvinyl alcohol (PVA) is widely recognized for its biocompatibility and non-toxic nature,<sup>23</sup> making it an ideal material for biomedical applications.<sup>24</sup> In the recyclable  $\text{MoS}_2$ /PVA sensor fabrication,  $\text{MoS}_2$  is incorporated within the PVA matrix, ensuring that  $\text{MoS}_2$  material does not come in contact with the skin. This embedding of  $\text{MoS}_2$  in the PVA matrix minimizes the potential biocompatibility concerns because PVA acts like a protective cover, eliminating any adverse interaction between  $\text{MoS}_2$  and biological tissues. Finally, the transience test shows that the  $\text{MoS}_2$ /PVA sensor dissolves in 300 s. Comparison of the performance of the fabricated recyclable  $\text{MoS}_2$ /PVA sensor with the original  $\text{MoS}_2$ /PVA pressure sensor reveals a negligible difference in temporal response. Under a constant pressure of 1 kPa, the recycled sensor exhibited a 10% change in current response compared to the original sensor. Furthermore, the resistance of two recycled water-soluble  $\text{MoS}_2$ /PVA sensors was monitored over 90 days and compared to the resistance of the original  $\text{MoS}_2$ /PVA sensor. The water soluble and recyclable  $\text{MoS}_2$ /PVA sensor are designed to address the critical challenge of electronic waste (e-waste). Unlike traditional sensors, this recyclable sensor offers an eco-conscious solution by enabling environmentally friendly disposal and reuse. The hydrophilic nature of the PVA substrate dissolves in DI water, eliminating persistent waste while allowing for efficient recovery of  $\text{MoS}_2$  material. This recyclability supports multiple fabrication cycles, making the process cost effective and enhancing sustainable. This  $\text{MoS}_2$ /PVA sensor provides a scalable, energy-efficient, and environmentally friendly alternative to conventional  $\text{MoS}_2$  based devices by combining temporary functionality with recyclability. This makes it ideal for recyclable or disposable electronics, biomedical sensors, and eco-friendly environmental monitoring, aligning with global effects to reduce resource consumption and waste in electronics.



## Experimental section

The water-soluble pressure sensor composed of recycled  $\text{MoS}_2$  functional material is fabricated through a two-step process. First, 2D  $\text{MoS}_2$  material is synthesized using a facile hydrothermal method. Subsequently,  $\text{MoS}_2$  liquid is combined with a water-soluble PVA polymer to form a recycled  $\text{MoS}_2$ /PVA thin film, with copper contacts attached to the  $\text{MoS}_2$ /PVA thin film used for pressure sensing applications. Informed consent was obtained for the experiments involving human participants.

### Materials

Polyvinyl alcohol ( $M_w$ : 61 000  $\text{g mol}^{-1}$ , 98.0–98.8 mol% hydrolysis), sodium molybdate ( $\text{Na}_2\text{MoO}_4$ ), and L-cystine were procured from SRL and Sigma Aldrich chemicals. During the synthesis, 0.01 M HCl was utilized. The morphology of  $\text{MoS}_2$  and  $\text{MoS}_2$ /PVA films was analysed using field electron scanning electron microscopy (FESEM, FEI Apreo Lovac). The chemical composition of synthesized  $\text{MoS}_2$  analyses was performed using XPS (Thermo Fisher Scientific K-Alpha XPS system). The electrical characteristics of the  $\text{MoS}_2$ /PVA sensor and the recycled  $\text{MoS}_2$ /PVA sensor were evaluated using a Keithley 2450 source meter.

### $\text{MoS}_2$ synthesis

The synthesis of 2D  $\text{MoS}_2$  material was achieved through a facile hydrothermal method, utilizing sodium molybdate and L-cystine precursors. The synthesis begins by dissolving sodium molybdate of 300 mg in 20 mL of DI water and sonicating for 15 min. Similarly, 300 mg of L-cystine is mixed with 50 mL of DI water and subjected to ultrasonication for 10 min to obtain a transparent solution. Subsequently, both prepared solutions are thoroughly

mixed using a magnetic stirrer for 30 min. To maintain a pH of 6.5, HCl is added to the mixed solution. Finally, the thoroughly mixed solution is transferred to an autoclave and maintained at 200 °C for 16 h, followed by natural cooling. The resulting solution is centrifuged at 4000 rpm for 30 min to collect the  $\text{MoS}_2$ , which is then stored in a dark place for further experiments. The synthesis of  $\text{MoS}_2$  is illustrated in Fig. 1.

### Fabrication of the $\text{MoS}_2$ /PVA sensor

The  $\text{MoS}_2$ /PVA sensors were fabricated using different concentrations of  $\text{MoS}_2$ /PVA solution (0.025 wt%, 0.125 wt%, 0.25 wt%, 0.375 wt%, 0.5 wt% and 0.6 wt%). The mixtures were continuously stirred for 6 h at 60 °C. Next, the thoroughly mixed solutions were poured into Petri dishes and kept in an oven at 60 °C for 6 h. The sensor fabrication processes are illustrated in Fig. 1. However, a uniform  $\text{MoS}_2$ /PVA film only formed above 0.375 wt%. The formed film (0.5 wt%) in the Petri dish after heating in oven is depicted in Fig. S1a of the ESI.† The carefully peeled  $\text{MoS}_2$ /PVA film is shown in Fig. S1b of the ESI.† The resulting films were cut into 1.5 cm  $\times$  1 cm dimensions. The copper wire was attached to the film with the help of silver paste, and later kept in oven at 60 °C for 3 h to make a strong bond between the  $\text{MoS}_2$ /PVA film and copper contacts. The sensor's flexibility did not significantly impact its performance. The  $\text{MoS}_2$ /PVA sensor fabrication process is scalable and compatible for mass production, making it suitable for industrial applications. Unlike other 2D material synthesis techniques, the hydrothermal process operates at lower temperatures and reduces the energy demands. Furthermore, the solution-casting processes avoid the need for complex vacuum systems or high-cost equipment, making it cost-effective and adaptable for large-area, high-throughput fabrication. The bending of the

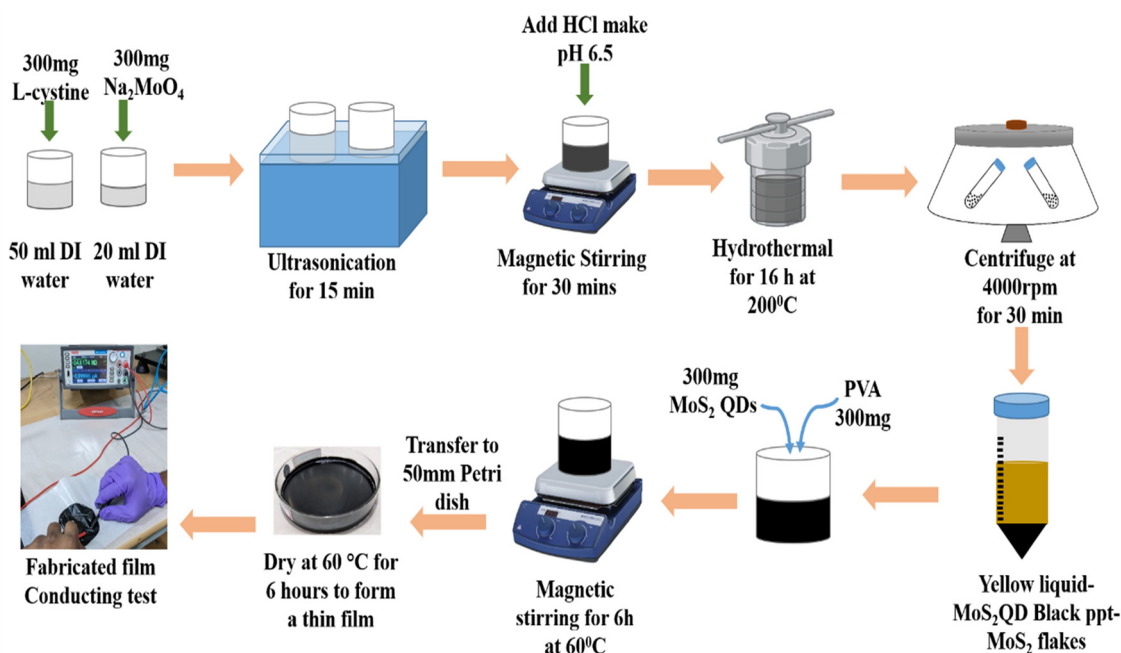


Fig. 1 Synthesis of 2D  $\text{MoS}_2$  and fabrication of the water-soluble  $\text{MoS}_2$ /PVA pressure sensor.



sensor with the copper wire attached using silver paste is shown in Fig. S1c of the ESI.† Moreover, the MoS<sub>2</sub>/PVA film exhibits the highest conductivity at 0.5 wt%. The comparison Table S1 (ESI†) of MoS<sub>2</sub>/PVA sensors at different concentrations and their resistivity values are included in ESI.†

### Characterization

A facile hydrothermal method was employed to synthesize the MoS<sub>2</sub> material. The resulting MoS<sub>2</sub> material and fabrication of MoS<sub>2</sub>/PVA sensor morphology was validated by scanning electron microscopy (SEM), the chemical composition of MoS<sub>2</sub> was analyzed using XPS spectroscopy, the crystalline structure was analyzed using XRD, and chemical bonds were identified using Raman spectroscopy. Fig. 2 illustrates the detailed material characterization of MoS<sub>2</sub> and MoS<sub>2</sub>/PVA sensors. The SEM image of synthesized MoS<sub>2</sub> showcases a flower like morphology consisting of hollow microspheres (Fig. 2a).<sup>25</sup> Fig. 2b shows the morphology of the fabricated MoS<sub>2</sub>/PVA pressure sensor. The prepared MoS<sub>2</sub> chemical composition was determined using Raman analysis. The conformation of prominent peaks identified at 408 cm<sup>-1</sup> and 383 cm<sup>-1</sup> (Fig. 2c) corresponds to A<sub>1g</sub> (out-of-plane vibration) and E<sub>1g</sub> (in-plane vibration) modes, respectively.<sup>26</sup> XRD analysis for virgin MoS<sub>2</sub> and recycled MoS<sub>2</sub> showed that the peak position is largely identical, confirming the

unchanged crystalline nature after recycling. X-ray diffraction (XRD) analysis of MoS<sub>2</sub> referenced against JCPDS no. 37-1492 confirms its hexagonal crystal structure. The characteristic peaks for virgin MoS<sub>2</sub> and recycled MoS<sub>2</sub> are at the (002), (100), (103), and (110) planes (Fig. 2d), which validates the material's crystalline phases. However, there is additional peak at 19.44° (101) in recycled MoS<sub>2</sub>, which is attributed to residual PVA. The MoS<sub>2</sub>/PVA composite's mechanical performance was assessed using tensile testing. Fig. 2e shows the standard composite MoS<sub>2</sub>/PVA stress-strain curve. Young's modulus is represented by the slope of the elastic deformation zone. Young's modulus, also known as the modulus of elasticity, indicates the stiffness and capacity of MoS<sub>2</sub>/PVA samples to tolerate deformation under tension, whereas the tensile strength in this instance indicates the highest stress that the MoS<sub>2</sub>/PVA thin film can sustain under stretching before failing. The ratio of the modified length to the original length following the breakage of the MoS<sub>2</sub>/PVA sample is known as the strain to failure (or elongation at break). A tensile strength of about 20 MPa and a Young's modulus of about 400 MPa are indicated by the elastic area (5%), which is visible on the stress strain curve.<sup>27,28</sup>

X-ray photoelectron spectroscopy (XPS) analysis was performed to analyze the chemical components of MoS<sub>2</sub>. Fig. 3a displays the full survey spectrum of MoS<sub>2</sub>, revealing the presence of Mo, S, C,

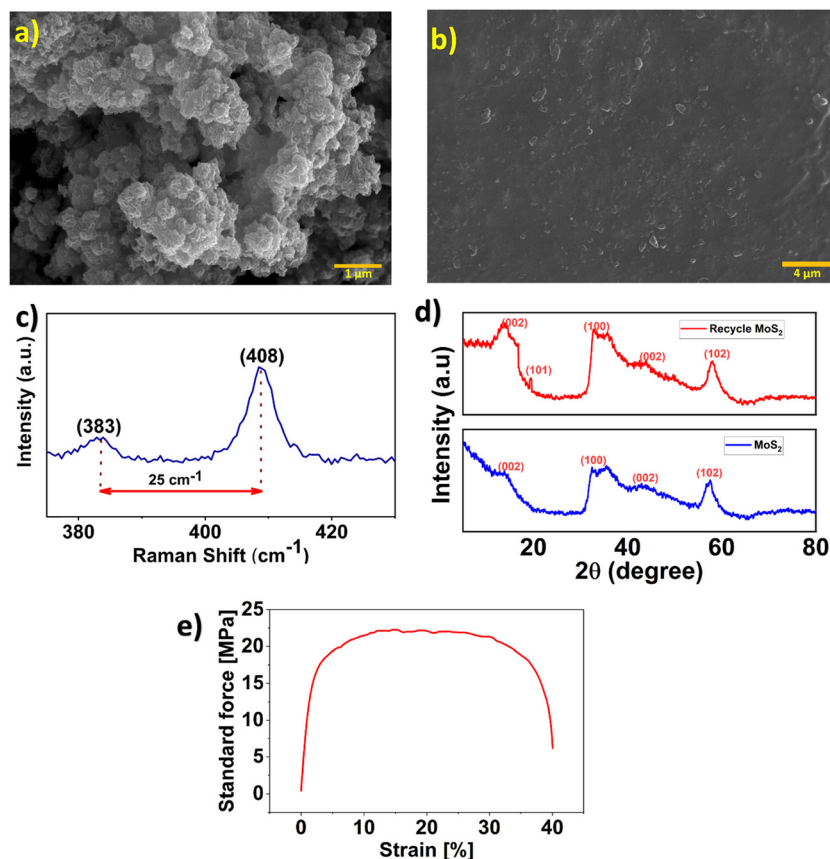


Fig. 2 Structural and mechanical characteristics of the MoS<sub>2</sub> and MoS<sub>2</sub>/PVA sensors. (a) FESEM image of synthesized MoS<sub>2</sub>, showcasing a flower-like morphology consisting of hollow microspheres. (b) Morphology of the fabricated MoS<sub>2</sub>/PVA sensor. (c) Raman spectra of synthesized MoS<sub>2</sub> with peaks ranging between 378 and 470 cm<sup>-1</sup>. (d) XRD spectra of both virgin MoS<sub>2</sub> and recycled MoS<sub>2</sub>. (e) Stress-strain curve of the fabricated MoS<sub>2</sub>/PVA sensor.





and O elements. The Mo 3d spectrum shows the two distinctive peaks at 229 eV ( $\text{Mo}^{4+} 3d_{5/2}$ ) and 232 eV ( $\text{Mo}^{4+} 3d_{3/2}$ ) (Fig. 3b), indicative of the  $\text{Mo(IV)}$  oxidation state of  $\text{MoS}_2$ . Meanwhile, another peak at 235.7 eV corresponds to the  $\text{Mo}^{6+}$  state of  $\text{MoO}_3$ . Additionally, a faint peak at 226.1 eV is attributed to S 2s. Furthermore, two prominent peaks at 161.8 eV and 163 eV (Fig. 3c) correspond to the binding energies of S  $2p_{1/2}$  and S  $2p_{3/2}$  for  $\text{S}^{2-}$ .<sup>29</sup> The peak around 531.2 eV (Fig. 3d) corresponds to O 1s. The primary reason for the O 1s peak in the  $\text{MoS}_2$  survey spectrum is due to partial oxidation of  $\text{MoS}_2$  when exposed to air.<sup>30,31</sup> The above characterization results confirm the formation of  $\text{MoS}_2$  using a facial hydrothermal method.

### Pressure sensing

The fabricated  $\text{MoS}_2/\text{PVA}$  sensor performance was evaluated by applying different pressures between 1–3 kPa. The water-soluble flexible pressure sensor was developed by combining  $\text{MoS}_2$  with polyvinyl alcohol (PVA) with copper wire contacts. The fabricated film was cut into length ( $L$ ) and width ( $W$ ) of 1.5 cm and 1 cm and with the help of silver paste copper wires connected to the sensor. The fabricated pressure sensor electrical response was measured using a Keithley source meter. The  $I$ - $V$  characteristics at different pressures and linearity between currents and voltages indicates that the fabricated sensor is a piezoresistive type and resistance decreases with applied external pressure between 1–3 kPa (Fig. 4a). A constant working voltage of 1 V is applied to the sensor to measure its current response. A constant pressure of 1 kPa is applied on the sensor (Fig. 4b). The sensor current response increased with the application of constant pressure, with the sensor current response recovering to the initial state of  $4.92 \times 10^{-7}$  A upon the release of the external pressure. The fabricated flexible

$\text{MoS}_2/\text{PVA}$  pressure sensor is subjected to different external pressures in the 1–3 kPa range (Fig. 4c). The sensor resistance decreases with increasing pressure, which eventually increases the current intensity. The response sensitivity of the fabricated piezoresistive sensor is generally represented as  $\frac{\Delta R/R}{\Delta p}$ , where  $p$  is the applied pressure, and  $\Delta R/R$  is the relative change of resistance upon applying the pressure. Three  $\text{MoS}_2/\text{PVA}$  sensors were tested and the  $\text{MoS}_2/\text{PVA}$  pressure sensor's sensitivity was calculated. The results illustrate consistent response trends across  $\text{MoS}_2/\text{PVA}$  sensors, which suggests good reproducibility. There were minute variations in the sensor's performance, which can be attributed to processing conditions. The sensitivity and coefficient of determination of the three  $\text{MoS}_2/\text{PVA}$  sensors are approximately  $0.87 \text{ kPa}^{-1}$  and 0.994, respectively.<sup>10,32</sup> Fig. 4d illustrates the sensitivity and coefficient of determination ( $R^2$ ) of fabricated  $\text{MoS}_2/\text{PVA}$  sensors. The rise time and fall time of the sensor signal response are significant (Fig. 4e and f). The sensor signal response rise from 10% to 90% is called the rise time. In contrast, the sensor signal response falls from 90% to 10% and is called the fall time. The rise and fall time are 260 ms and 320 ms, respectively. The fabricated sensor underwent a cyclic test to further demonstrate the performance (Fig. 4g). The current response shows a negligible change for 1200 loading and unloading cycles, which was well retained over multiple cycles. The resistance of two water-soluble  $\text{MoS}_2/\text{PVA}$  sensors was tested continuously for 90 days, and a negligible change in the resistance response was observed (Fig. 4h). Hysteresis analysis was performed on the fabricated  $\text{MoS}_2/\text{PVA}$  recyclable sensor to evaluate the response under loading and unloading conditions. The recyclable  $\text{MoS}_2/\text{PVA}$  sensor shows minimal hysteresis, indicating its high reliability and repeatability in pressure sensing.

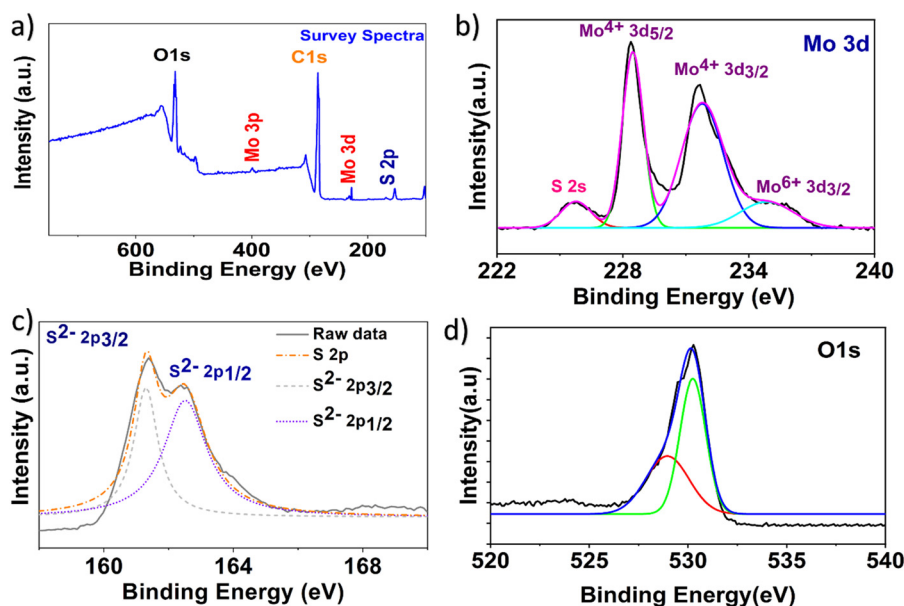


Fig. 3 XPS analysis of the prepared  $\text{MoS}_2$  material. (a) Survey spectrum of synthesized  $\text{MoS}_2$ . (b) The Mo  $3d_{5/2}$  and Mo  $3d_{3/2}$  peaks are centered at 229 eV and 232 eV, respectively. (c) The peaks of S  $2p_{3/2}$  and S  $2p_{1/2}$  are centered at 161.8 eV and 163 eV, respectively. (d) Oxygen spectrum showing a peak at 531.2 eV.



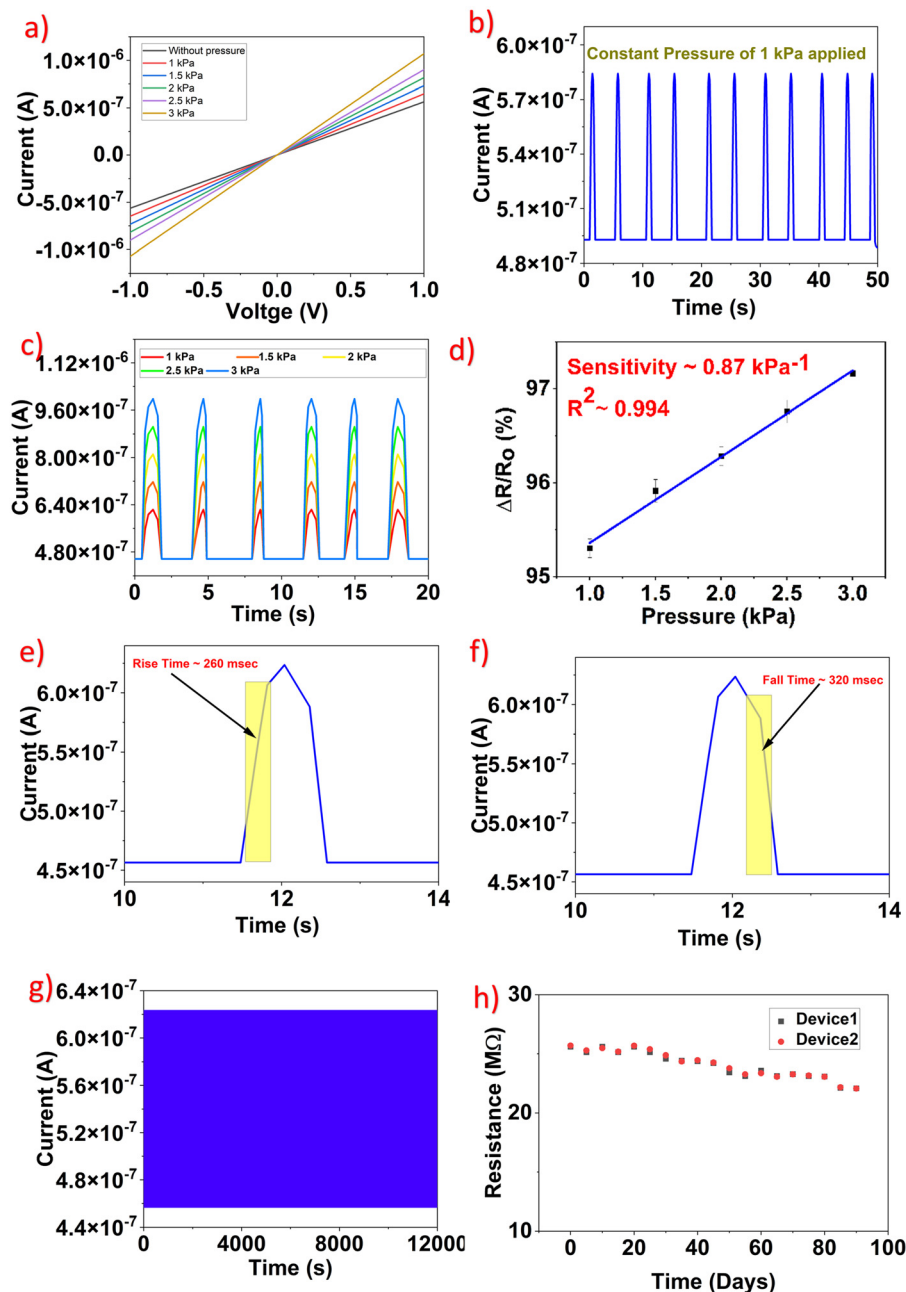


Fig. 4 Performance evaluation of the recyclable  $\text{MoS}_2/\text{PVA}$  sensor under different pressures. (a)  $I$ - $V$  characteristics of the  $\text{MoS}_2/\text{PVA}$  pressure sensor at different pressures. (b) Constant pressure of 1 kPa applied to the fabricated sensor. (c) Pressure sensor response increase at different pressures. (d) The calculated sensitivity of three sensors is approximately  $0.87 \text{ kPa}^{-1}$  with a coefficient of determination ( $R^2$ ) of 0.994. (e) Calculated rise time of 260 ms. (f) Calculated fall time of 320 ms for the fabricated sensor signal response. (g) Durability of the  $\text{MoS}_2/\text{PVA}$  pressure sensor tested for 1200 cycles. (h) Response of the sensor resistance of two devices over 3 months.

The hysteresis graph is presented in Fig. S2 of the ESI†. Finally, a humidity test was conducted for the fabricated  $\text{MoS}_2/\text{PVA}$  sensor to check whether the sensor was affected by the surrounding environment. The humidity test was conducted in a humidity chamber. There was negligible change in the performance of the sensor under normalized resistance (Fig. S3 in ESI†).

The sensing mechanism of the fabricated sensor is the modulation of the distance of  $\text{MoS}_2$  flakes upon external

pressure. This mechanism is schematically depicted in Fig. 5. The conducting  $\text{MoS}_2$  flakes are covered with polymer on both sides, forming a resistive film. When no pressure is applied, the distance ( $d_1$ ) between the  $\text{MoS}_2$  flakes remains unchanged (Fig. 5, schematic I), resulting in no alteration in current response and resistance. However, the distance ( $d_2, d_3$ ) between  $\text{MoS}_2$  flakes is reduced and is close to the tunnelling distance between the two flakes upon the applied pressure to the sensor.



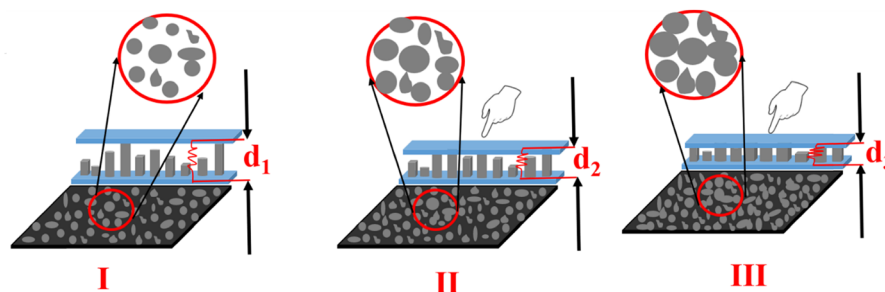


Fig. 5 (I)–(III) Sensing mechanism of the fabricated water-soluble MoS<sub>2</sub>/PVA sensor.

As a result, the charge carriers (electrons) tunnel between them. This reduced distance leads to a decrease in resistance within the MoS<sub>2</sub>/PVA pressure sensor, enabling higher flow of current. Here, the change in resistance of the sensor directly correlates with the applied pressure. Additionally, water soluble PVA serves as an important component in the fabrication process, acting as a binder to hold the MoS<sub>2</sub> flakes together and providing mechanical stability to the pressure sensor. Furthermore, the flexibility of PVA allows the sensor to undergo deformation under applied pressure and ensures that the distance between the flakes can be effectively modulated by external pressure. Therefore, the combination of MoS<sub>2</sub> flakes and PVA polymer contribute to the exceptional performance of the pressure sensor in a pressure sensing application.

#### Applications of the fabricated MoS<sub>2</sub>/PVA pressure sensor

The water-soluble flexible MoS<sub>2</sub>/PVA pressure sensor was utilized for real-time applications owing to its outstanding pressure sensing results like a sensitivity of 0.87 kPa<sup>-1</sup>, excellent durability

over 1200 cycles, and stable performance. Initially, it was utilized for detecting air pressure from a bulb syringe, and it later proved effective in capturing various physiological signals from the human body. Subsequently, it was used as directional keys (left, right, up, and down) for a handheld game console. The pressure sensor was attached to an acrylic sheet. Its contacts are connected to the probes of a source meter to detect the current response. The resulting current response was observed when the air was squeezed and released onto the MoS<sub>2</sub>/PVA sensor using the bulb syringe. Fig. 6 illustrates the positioning of the bulb syringe at three different distances from the sensor: 1 cm, 3 cm, and 5 cm. Remarkably, the sensor demonstrated the ability to detect air from various distances, with corresponding changes in the magnitude of the signal response. At a distance of 1 cm, the current response exhibited a higher magnitude due to the higher pressure of air. Conversely, the magnitude of the current response decreased as the distance increased from 1 cm to 5 cm. This experiment highlighted the sensor's capability to detect changes in the pressure of air, and

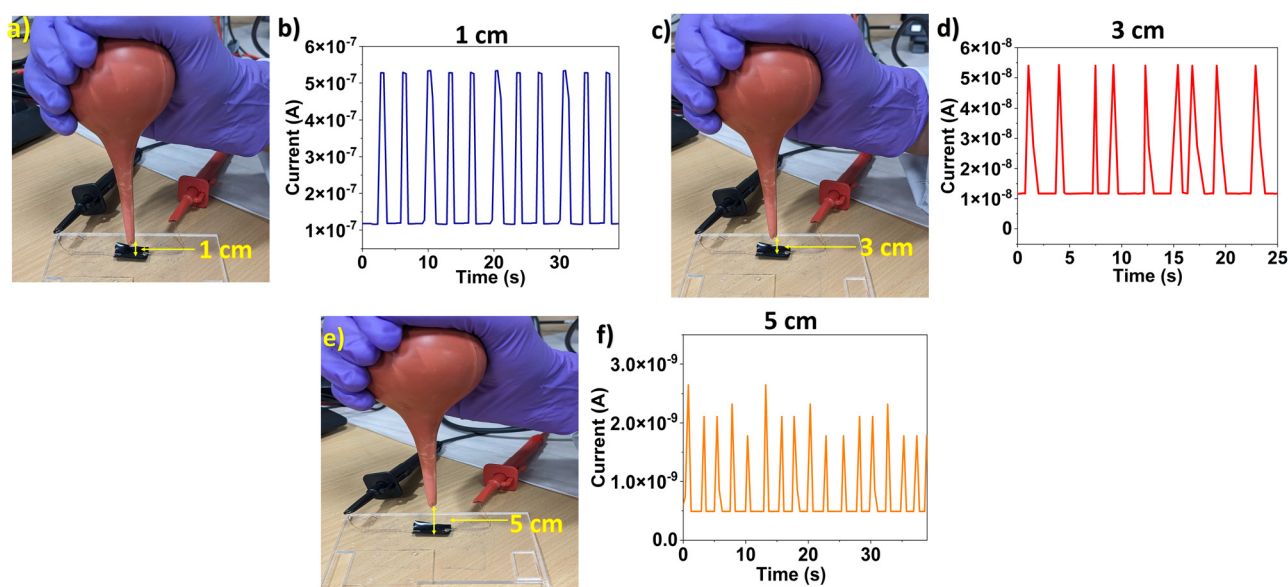


Fig. 6 Recyclable MoS<sub>2</sub>/PVA sensor for detection of bulb syringe air at varying distances. (a–b) Bulb syringe air detected by the water-soluble MoS<sub>2</sub>/PVA pressure sensor at a distance of 1 cm, (c–d) 3 cm, and (e–f) 5 cm.



this feature is required for applications that demand sensitivity to minute changes in airflow.

The fabricated  $\text{MoS}_2/\text{PVA}$  pressure sensor was integrated with a bandage to provide mechanical support and facilitate practical application in detecting arterial pulses. The central part of bandage supports the  $\text{MoS}_2/\text{PVA}$  sensor, while the two ends of the bandage support copper electrodes. The sticky nature of the two ends of the bandage ensures that the sensor electrodes are securely adhered, providing mechanical strength and stability. This configuration allows for a reliable connection of the probes from the source meter, ensuring an accurate and consistent pressure sensing during real time application. The setup is particularly effective for detecting artery pulses in the hand carotid artery pulses in the neck. The carotid pulse plays a crucial role in blood circulation, offering vital insights into the body circulatory system. Many specialized biomedical technologies currently rely on expensive, bulky, and uncomfortable instruments, limiting their practical applications. However, the water-soluble  $\text{MoS}_2/\text{PVA}$  pressure sensor offers a cost-effective and straightforward alternative for monitoring real-time carotid arterial pulse signals. The sensor was installed on the subject's artery to record the pulses (Fig. 7a) and the inset Figure depicts the  $\text{MoS}_2/\text{PVA}$  sensor attached to the bandage for support. The  $\text{MoS}_2/\text{PVA}$  pressure sensor detected artery pulses (Fig. 7b). Fig. 7c shows the artery pulse exhibiting three peaks labelled as P1, P2, and P3.<sup>33</sup> Subsequently, the flexible and easily conformable fabricated water-soluble  $\text{MoS}_2/\text{PVA}$  sensor was employed to capture the radial artery pulse from the left hand (Fig. 7d). The arterial pulse is a peripheral signal used to assess cardiovascular health. This signal detected by the  $\text{MoS}_2/\text{PVA}$  sensor is depicted in Fig. 7e. The arterial pulse is commonly employed for measuring blood pressure. A typical pulse wave is depicted

in Fig. 7f, marked with A, P, V, and D. Here, A represents the baseline, P indicates the percussion wave, V signifies the valley, and D denotes the dicrotic wave.<sup>34,35</sup>

The fabricated sensor serves to sense signals from the human body and can be used as directional keys for the game console (Fig. 8). Fig. 8(a) and (b) illustrate using the sensor to play a Mario game, where pressing the upward direction key causes Mario to jump. To integrate the sensor into the gaming console, foam was cut into four square pieces measuring  $2\text{ cm} \times 2\text{ cm}$  to provide support for the fabricated sensor. The  $\text{MoS}_2/\text{PVA}$  pressure sensor was then attached to these foam pieces along with its contacts. Each of the four sensor contacts was connected to the game console, allowing the sensors to function as directional keys. The latency of the fabricated  $\text{MoS}_2/\text{PVA}$  sensor was approximately 420 ms when subjected to external pressure. This setup enabled effective and responsive interactions with the game console, demonstrating the practical application of the  $\text{MoS}_2/\text{PVA}$  pressure sensor in gaming.

Fig. 9a–d displays a series of images depicting the fabricated  $\text{MoS}_2/\text{PVA}$  sensor dissolved in DI water for  $\sim 300\text{ s}$ . The sensor is placed in a Petri dish filled with DI water (Fig. 8a). Water-soluble PVA reacts with DI water and gradually disintegrates after 100 s (Fig. 9b and c). Finally, Fig. 9d illustrates the complete dissolution of PVA in DI water, leaving behind traces of  $\text{MoS}_2$ . The dissolution of the sensor is due to the hydrophilic nature of polyvinyl polymer chains of hydroxyl ( $-\text{OH}$ ) groups. When the  $\text{MoS}_2/\text{PVA}$  sensor comes in contact with DI water, the water molecules interact with the hydroxyl groups through hydrogen bonding. These interactions weaken the intermolecular forces holding the polymer chain together, eventually causing them to separate and dissolve in the water, leaving  $\text{MoS}_2$  traces in DI water. The highly transient feature of our

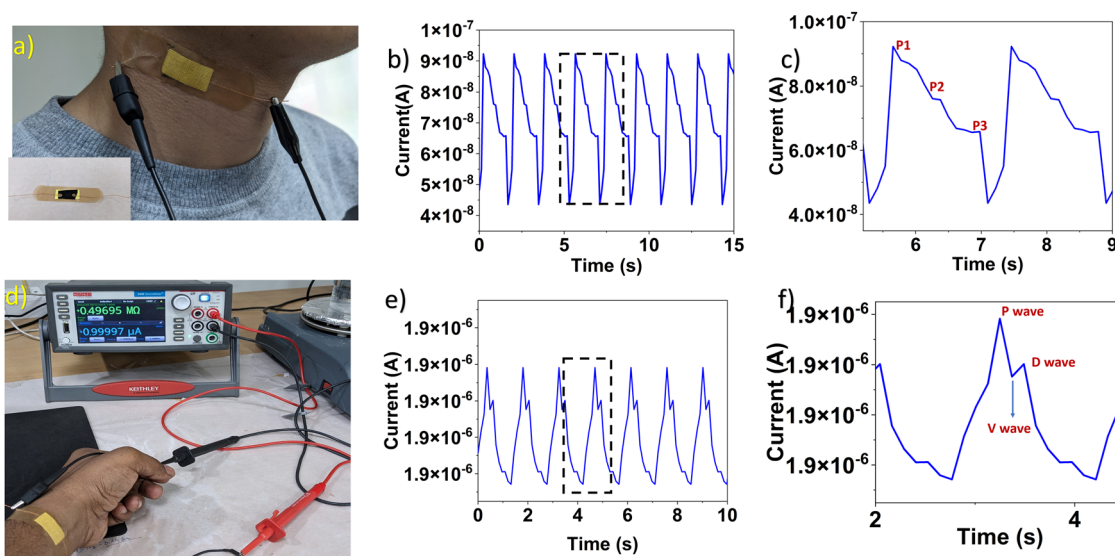


Fig. 7 The  $\text{MoS}_2/\text{PVA}$  sensor utilized for arterial pulse detection. (a) Fabricated sensor affixed to the neck with the help of a bandage; the inset shows the pressure sensor attached to the bandage. (b) and (c) Carotid arterial pulse (neck) detected by the fabricated pressure sensor. (d)–(f) Radial artery pulse (hand) detected by the  $\text{MoS}_2/\text{PVA}$  pressure sensor.





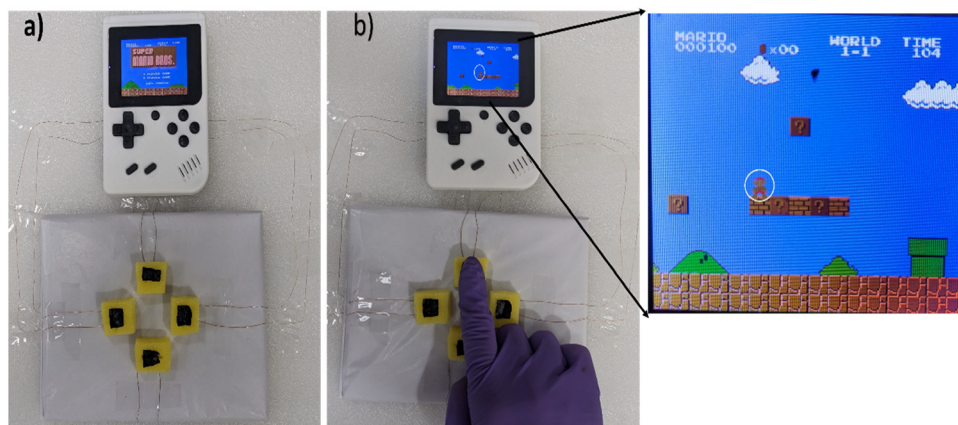


Fig. 8 Demonstration of recycled  $\text{MoS}_2$ /PVA pressure sensor keys for Mario game application. (a) Directional  $\text{MoS}_2$ /PVA keys connected to the gaming console. (b) Playing the Mario game by pressing the upward directional  $\text{MoS}_2$ /PVA sensor key.

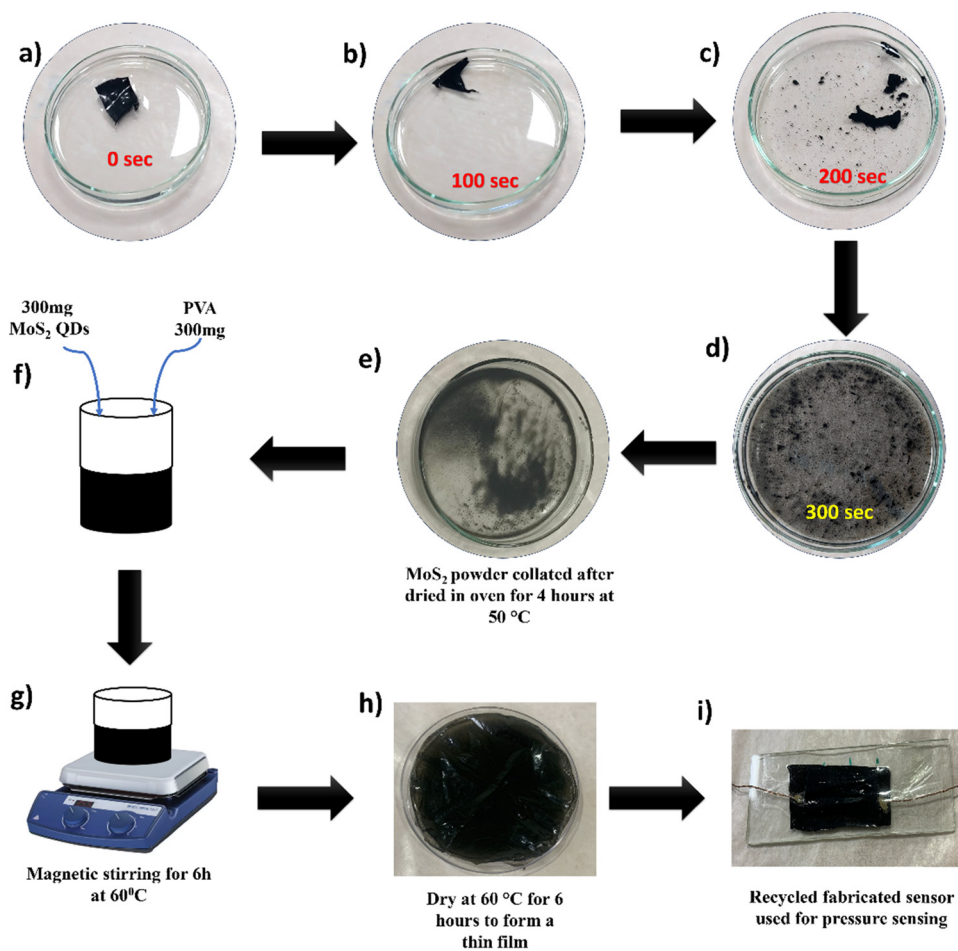


Fig. 9 Dissolution and recycling process of the  $\text{MoS}_2$ /PVA sensor. (a)–(d) Sequence of images illustrating the dissolution of the fabricated sensor in water, which completely dissolves in  $\sim 300$  s, with the functional material  $\text{MoS}_2$  powder remaining on the surface of the Petri dish. (e)  $\text{MoS}_2$  powder collected after being dried in an oven. (f)–(i) The recycled  $\text{MoS}_2$ /PVA pressure sensor fabrication process.

fabricated recyclable  $\text{MoS}_2$ /PVA sensor is manifested by its quick dissolution in DI water. The fabricated  $\text{MoS}_2$ /PVA sensor dissolves within 300 s, showing its rapid transient nature

compared with other literature utilizing similar materials for transient electronics. A table comparing the transient time between different sensors with our fabricated  $\text{MoS}_2$ /PVA sensor



is shown in Table S2 in the ESI.† During the transience test, the sensor completely dissolved in deionized (DI) water, leaving the functional material, MoS<sub>2</sub>, at the bottom of the Petri dish. The MoS<sub>2</sub> solution was dried by placing the Petri dish in an oven at 60 °C. The resulting MoS<sub>2</sub> powder was collected and washed with DI water and placed back in the oven at 60 °C. This process was repeated three times to ensure the removal of any contaminants. Finally, the recycled MoS<sub>2</sub>/PVA sensor was fabricated using the collected MoS<sub>2</sub> powder, following the same fabrication process shown in Fig. 9e–i.

Fig. 10a shows the temporal response of the recycled MoS<sub>2</sub>/PVA sensor under a constant pressure of 1 kPa. The sensitivity calculated for the original and recycled sensor showed 10% deviation. The calculated sensitivity of the recycled MoS<sub>2</sub>/PVA sensor along with the coefficient of determination is shown as Fig. S4 of the ESI.† The 10% current deviation in the recycled sensor is considered “negligible” because this level of variation does not significantly impact the sensor's functionality for the specific application targeted. Unlike absolute current measurements, the MoS<sub>2</sub>/PVA sensor operates based on the relative change in current upon applied pressure. Thus, 10% deviation is negligible because the sensor's core function (detecting and responding to pressure changes) remains unaffected, making it suitable for the intended application. Additionally, the resistance of two recycled water-soluble MoS<sub>2</sub>/PVA sensors was tested for 90 days and compared with the resistance of the original MoS<sub>2</sub>/PVA sensor resistance. There is a negligible change in the resistance response of the recycled MoS<sub>2</sub>/PVA and original MoS<sub>2</sub>/PVA sensor results (Fig. 10b).

### State of the art

In recent years, research efforts have significantly intensified in focusing on developing flexible pressure sensors due to their versatile applications in areas like healthcare monitoring, human–computer interaction, wearable electronics, and robotics.<sup>36</sup> Zhao *et al.*<sup>37</sup> presents a flexible pressure sensor using a laser-induced graphene. The sensor is designed with a simple and efficient fabrication process, utilizing LIG electrodes and a dielectric layer. The sensor achieves a wide working range from 0 Pa to 10.4 kPa, detection limit as low as 1.2 Pa, and high sensitivity

up to 2.52 kPa<sup>−1</sup>. The sensor's performance makes it suitable for various real-world applications, such as motion detection and health monitoring, demonstrating excellent stability and responsiveness.<sup>37</sup> Similarly, Guan *et al.*<sup>38</sup> introduced a novel, scalable method for transforming natural wood into a flexible pressure sensor with high sensitivity and stability. The process involves converting rigid wood into flexible wood (FW) through chemical treatment and enhancing its conductivity by coating it with reduced graphene oxide (rGO). The resulting FW/rGO-based pressure sensors exhibit impressive performance, including a high sensitivity of 1.85 kPa<sup>−1</sup>, a broad linear range up to 60 kPa, and excellent durability over 10 000 cycles.<sup>38</sup> In another work, Cao *et al.*<sup>39</sup> developed a novel pressure-sensing material inspired by human skin's dual mechanoreceptors. The authors designed 3D printed laminated graphene materials with ultra-thin and thick-walled cellular microstructures to achieve a piezoresistive pressure sensor. The laminated graphene structure allows for the creation of flexible pressure sensing arrays, showing potential applications in monitoring physiological signals, electronic skin, and human–machine interfaces.<sup>39</sup> Yang *et al.*<sup>40</sup> fabricated a flexible pressure sensor based on MXene/polyurethane (PU) with a spinosum structure, created using a cost-effective spray method. The sensor exhibits exceptional sensitivity, with rapid response and recovery times, and remarkable durability over 10 000 cycles. Its unique self-healing ability is derived from the hydrogen bonds in PU, allowing it to recover functionality after mechanical damage.<sup>40</sup> Huang *et al.*<sup>41</sup> developed a highly sensitive and flexible pressure sensor that utilizes a randomly distributed columnar array structure to achieve a wide linear pressure response range. The sensor was fabricated using aerosol printing and sandpaper inversion techniques and features a bilayer contact-resistive structure with a flexible interdigital electrode as the active layer. The sensor demonstrates high sensitivity (38.25 kPa<sup>−1</sup>), a fast response time (43 ms), and excellent stability across a pressure range of 0 to 128 kPa. Its potential applications include monitoring human physiological signals like pulse and sound vibration, making it suitable for wearable health monitoring and robotics.<sup>41</sup> Li *et al.*<sup>42</sup> introduced a highly sensitive pressure sensor utilizing a sponge-like structure composed of PDMS,

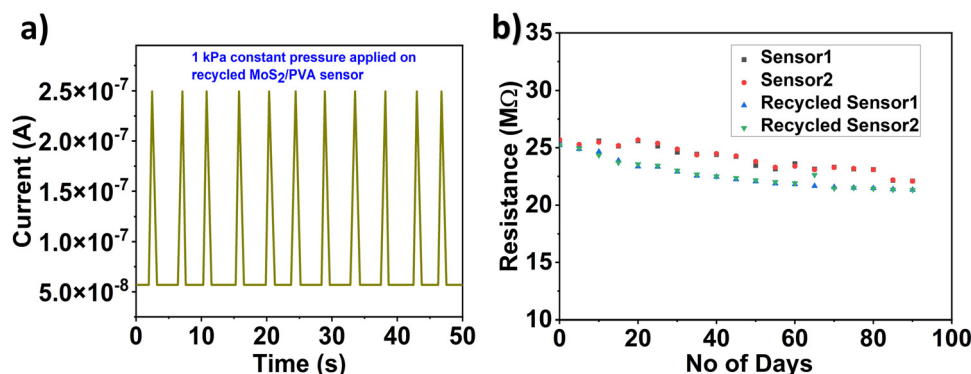


Fig. 10 Performance evaluation of the recycled MoS<sub>2</sub>/PVA sensor. (a) Constant pressure of 1 kPa applied to the recycled MoS<sub>2</sub>/PVA sensor. (b) Response of the sensor resistance of two devices (MoS<sub>2</sub>/PVA sensors) and two devices (recycled MoS<sub>2</sub>/PVA sensors) over 3 months.



**Table 1** Comparison of various fabricated sensors with the recyclable MoS<sub>2</sub>/PVA sensor

S. no.	Material	Substrate	Applications	Reusable	Cite
1	Laser-induced graphene (LIG)	Polyimide (PI) paper	Health monitoring and motion detection	No	37
2	rGO	Flexible wood (FW) substrate	Wearable electronics and electronic skins	No	38
3	RGO	Polydimethylsiloxane (PDMS)	Electronic skin	No	39
4	MXene	Polyurethane (PU), polyimide (PI)	Human-activity monitoring	No	40
5	Ecoflex00-30, multi-walled carbon nanotubes (MWCNTs), PEDOT, silver nanoparticles	Polyimide (PI), polydimethylsiloxane (PDMS)	Human physiological signals	No	41
6	Nitrogen-doped graphene nanosheets (N-GNS), liquid metal (LM)	Polydimethylsiloxane (PDMS)	Monitoring of human activities	No	42
7	Titanium (Ti) and silver (Ag)	Polydimethylsiloxane (PDMS)	Monitoring human pulse waves	No	43
8	Mxene	VHB tape	Human physiological signals	No	44
9	MoS <sub>2</sub>	PVA	Healthcare and consumer electronic	Yes	This work

liquid metal, and nitrogen-doped graphene nanosheets. The sensor is designed for wearable health monitoring and can detect small pressure changes with high sensitivity, rapid response, and recovery times. The integration of liquid metal into the sponge structure enhances the sensor's performance by improving charge transfer at the interface, making it capable of real-time monitoring of human activities like pulse, skin pressure, and throat movements.<sup>42</sup> Yue *et al.*<sup>43</sup> fabricated an ultra-sensitive pressure sensor. The sensor is constructed using large alveolar deep tooth electrodes combined with a stretchable, oriented thermoplastic polyurethane serving as an isolation layer. This design enhances the sensitivity and broadens the linear range of the sensor, achieving an ultra-high sensitivity of 230 kPa<sup>-1</sup> between 1.1 to 100 kPa.<sup>43</sup> Lv *et al.*<sup>44</sup> presents a flexible pressure sensor using a wrinkle-structured MXene film. The wrinkle structure enables the sensor to achieve exceptional performance, including a high sensitivity of approximately 860 kPa<sup>-1</sup> and a detection range from 0.5 Pa to 30 kPa. The sensor also exhibits rapid response and recovery times and high stability over 11 600 cycles. This makes it highly suitable for real-time monitoring of small motions, such as human physiological signals, and various objects, showing significant potential for applications in wearable electronics, precision instruments, and human health monitoring.<sup>44</sup> A comparison of various fabricated sensors with a recyclable MoS<sub>2</sub>/PVA sensor is shown in Table 1. Even though researchers have employed novel materials to enhance the performance of pressure sensors, these materials often contribute to e-waste after their use. To address this issue, our developed MoS<sub>2</sub>/PVA sensor is designed to dissolve in water, allowing the MoS<sub>2</sub> to be recovered and recycled for the fabrication of new pressure sensors. This approach improves performance and promotes sustainability by reducing e-waste. The current recyclable MoS<sub>2</sub>/pressure sensor operation range of 1 kPa to 3 kPa aligns well with the requirements for subtle physiological monitoring, such as arterial pulse detection. Our sensor is designed for wearable, biomedical and gaming applications while existing industrial pressure sensors often operate in the tens to hundreds of kPa range for heavy-load sensing. A comparison table of current recycled MoS<sub>2</sub>/PVA sensors exhibiting exciting physiological signal monitoring are shown Table S3 in the ESI.†

The MoS<sub>2</sub>/PVA sensor exhibits good performance in flexible sensing applications and shows reusable characteristics of the fabricated sensor. However, key limitations must be addressed for broader applications. The main challenge of the fabricated MoS<sub>2</sub> sensor is its biodegradability, while PVA dissolves in DI water. Understanding the long term environmental impact is important, specifically for transient electronics. The next key challenge is providing stable electrical contacts since a strong adhesion between MoS<sub>2</sub> and contacts is crucial for durability without compromising flexibility. Another challenge is the lack of tunable degradation, and the fabricated sensor lifespan cannot be precisely controlled. Finally, a full-cycle study and waste management are necessary to evaluate disposal or recycling methods for the fabrication of sensors.

## Conclusion

This paper presents a promising recyclable pressure sensor incorporating 2D MoS<sub>2</sub> as the functional material and water-soluble polyvinyl alcohol (PVA) polymer. The developed recyclable pressure sensor presents a promising avenue for sustainable electronics. The fabricated sensor exhibits piezoresistive behavior and demonstrates good performance across various pressures, with excellent sensitivity of 0.87 kPa<sup>-1</sup> and durability. Moreover, the sensor versatility is showcased through its application in detecting radial and carotid artery pulses, monitoring air pressures, and serving as directional keys for a gaming console. Its stable performance over three months and successful application in real-time scenarios highlight its practicality and reliability. The ability to fully dissolve the sensor in water and fabricate a recycled version with negligible performance degradation underscores its potential for sustainable use. This innovative approach reduces material wastage and offers a viable solution for environmentally friendly wearable electronics, paving the way for future research and development in sustainable electronic devices.

## Author contributions

Naveen Bokka: conceptualization, data curation, formal analysis, investigation, methodology, visualization, writing – original



draft. Nongthombam Joychandra Singh: data curation, formal analysis, visualization, writing. Chandra Sekhar Reddy K.: methodology, writing – review and editing. Parikshit Sahatiya: supervision, formal analysis, funding, writing – review and editing.

## Data availability

The data supporting this article are included within the manuscript.

## Conflicts of interest

There are no conflicts to declare.

## Acknowledgements

PS acknowledges the Central Analytical Laboratory, BITS Pilani Hyderabad Campus, for assistance with material characterization.

## References

- 1 Z. Nazari and P. Musilek, Impact of digital transformation on the energy sector: a review, *Algorithms*, 2023, **16**(4), 211.
- 2 M. Javaid, A. Haleem, S. Rab, R. P. Singh and R. Suman, Sensors for daily life: a review, *Sens. Int.*, 2021, **2**, 100121.
- 3 N. Bokka, V. Selamneni, V. Adepu, S. Jajjara and P. Sahatiya, Water soluble flexible and wearable electronic devices: a review, *Flexible Printed Electron.*, 2021, **6**(4), 043006.
- 4 S. S. V. Vuppalladadiyam, B. S. Thomas, C. Kundu, A. K. Vuppalladadiyam, H. Duan and S. Bhattacharya, Can e-waste recycling provide a solution to the scarcity of rare earth metals? An overview of e-waste recycling methods, *Sci. Total Environ.*, 2024, **924**, 171453.
- 5 S. Manfredi, D. Tonini and T. H. Christensen, Contribution of individual waste fractions to the environmental impacts from landfilling of municipal solid waste, *Waste Manage.*, 2010, **30**(3), 433–440.
- 6 M. A. Mir and S. K. Chang, Saudi Arabia E-waste management strategies, challenges and opportunities, effect on health and environment: a strategic review, *Emerging Contam.*, 2024, 100357.
- 7 V. Forti, C. P. Baldé, R. Kuehr and G. Bel, *The global e-waste monitor 2020*, United Nations University (UNU), International Telecommunication Union (ITU) & International Solid Waste Association (ISWA), Bonn/Geneva/Rotterdam, 2020, p. 120.
- 8 N. Bokka, V. Selamneni and P. Sahatiya, A water destructible SnS 2 QD/PVA film based transient multifunctional sensor and machine learning assisted stimulus identification for non-invasive personal care diagnostics, *Mater. Adv.*, 2020, **1**(8), 2818–2830.
- 9 Y. Choi, J. Koo and J. A. Rogers, Inorganic materials for transient electronics in biomedical applications, *MRS Bull.*, 2020, **45**(2), 103–112.
- 10 N. Bokka, G. Khush Mahendrakumar and P. Sahatiya, A water-soluble micropatterned MoS<sub>2</sub> quantum dots/poly-vinyl alcohol film as a transient contact (pressure) and non-contact (humidity) as touch and proximity sensor, *J. Appl. Polym. Sci.*, 2022, **139**(9), 51711.
- 11 Z. Wei, Z. Xue and Q. Guo, Recent progress on bioresorbable passive electronic devices and systems, *Micromachines*, 2021, **12**(6), 600.
- 12 J. Xu, H. Guo, H. Ding, Q. Wang, Z. Tang, Z. Li and G. Sun, Printable and recyclable conductive ink based on a liquid metal with excellent surface wettability for flexible electronics, *ACS Appl. Mater. Interfaces*, 2021, **13**(6), 7443–7452.
- 13 N. X. Williams, G. Bullard, N. Brooke, M. J. Therien and A. D. Franklin, Printable and recyclable carbon electronics using crystalline nanocellulose dielectrics, *Nat. Electron.*, 2021, **4**(4), 261–268.
- 14 Y. Liu, H. Wang and Y. Zhu, Recycling of nanowire percolation network for sustainable soft electronics, *Adv. Electron. Mater.*, 2021, **7**(9), 2100588.
- 15 Y. Guo, S. Chen, L. Sun, L. Yang, L. Zhang, J. Lou and Z. You, Degradable and fully recyclable dynamic thermoset elastomer for 3D-printed wearable electronics, *Adv. Funct. Mater.*, 2021, **31**(9), 2009799.
- 16 T. Ye, F. Xiu, S. Cheng, C. Ban, Z. Tian, Y. Chen and W. Huang, Recyclable and flexible dual-mode electronics with light and heat management, *ACS Nano*, 2020, **14**(6), 6707–6714.
- 17 M. Tavakoli, P. Alhais Lopes, A. Hajalilou, A. F. Silva, M. Reis Carneiro, J. Carvalheiro and A. T. de Almeida, 3R Electronics: Scalable Fabrication of Resilient, Repairable, and Recyclable Soft-Matter Electronics, *Adv. Mater.*, 2022, **34**(31), 2203266.
- 18 N. Bokka, V. Adepu, A. Tiwari, S. Kanungo and P. Sahatiya, A detailed comparative performance analysis of the Transition Metal Di-chalcogenides (TMDs) based strain sensors through experimental realisations and first principle calculations, *FlatChem*, 2022, **32**, 100344.
- 19 R. Qin, X. Li, M. Hu, G. Shan, R. Seeram and M. Yin, Preparation of high-performance MXene/PVA-based flexible pressure sensors with adjustable sensitivity and sensing range, *Sens. Actuators, A*, 2022, **338**, 113458.
- 20 D. Thakur, C. Porwal, V. S. Chauhan, V. Balakrishnan and R. Vaish, 2D transition metal Dichalcogenides: Synthesis methods and their pivotal role in Photo, Piezo, and photo-piezocatalytic processes, *Sep. Purif. Technol.*, 2024, **337**, 126462.
- 21 N. Bokka, J. Karhade and P. Sahatiya, Deep learning enabled classification of real-time respiration signals acquired by MoSSe quantum dot-based flexible sensors, *J. Mater. Chem. B*, 2021, **9**(34), 6870–6880.
- 22 R. Wu, H. Zhang, H. Ma, B. Zhao, W. Li, Y. Chen and X. Duan, Synthesis, modulation, and application of two-dimensional TMD heterostructures, *Chem. Rev.*, 2024, **124**(17), 10112–10191.





- 23 M. Teodorescu, M. Bercea and S. Morariu, Biomaterials of poly(vinyl alcohol) and natural polymers, *Polym. Rev.*, 2018, **58**(2), 247–287.
- 24 E. S. Marín Cardona, J. J. Rojas Camargo and Y. A. Ciro Monsalve, A review of polyvinyl alcohol derivatives: promising materials for pharmaceutical & biomedical applications, *Afr. J. Pharm. Pharmacol.*, 2014, 674–684.
- 25 V. Selamneni, K. Gohel, N. Bokka, S. Sharma and P. Sahatiya, MoS<sub>2</sub>-Based Multifunctional Sensor for Both Chemical and Physical Stimuli and Their Classification Using Machine Learning Algorithms, *IEEE Sens. J.*, 2020, **21**(3), 3694–3701.
- 26 S. Siraj, G. Bansal, B. Hasita, S. Srungaram, S. K. S, F. J. Rybicki and P. Sahatiya, MXene/MoS<sub>2</sub> piezotronic acetone gas sensor for management of diabetes, *ACS Appl. Nano Mater.*, 2024, **7**(10), 11350–11361.
- 27 G. M. Janeesh, V. Meera, A. M. Shalom, D. Rajan Babu, N. A. Nambi Raj, M. S. Sreekanth and T. P. Sumangala, Enhanced electrical conductivity and structural, mechanical characterization of standalone poly(vinyl alcohol)-graphite nanoplatelets composite films, *J. Appl. Polym. Sci.*, 2021, **138**(10), 49976.
- 28 K. Iritani, A. Nakanishi, A. Ota and T. Yamashita, Fabrication of Novel Functional Cell-Plastic Using Polyvinyl Alcohol: Effects of Cross-Linking Structure and Mixing Ratio of Components on the Mechanical and Thermal Properties, *Global Challenges*, 2021, **5**(8), 2100026.
- 29 N. Bokka and P. Sahatiya, Heat and light triggered mechanical destruction of 2D materials based electronic devices fabricated on wax substrate, *FlatChem*, 2022, **35**, 100423.
- 30 T. R. Malagrino, A. P. Godoy, J. M. Barbosa, A. G. Lima, N. C. Sousa, J. J. Pedrotti and J. Taha-Tijerina, Multifunctional hybrid MoS<sub>2</sub>-PEGylated/Au nanostructures with potential theranostic applications in biomedicine, *Nanomaterials*, 2022, **12**(12), 2053.
- 31 F. J. Zhang, X. Li, X. Y. Sun, C. Kong, W. J. Xie, Z. Li and J. Liu, Surface partially oxidized MoS<sub>2</sub> nanosheets as a higher efficient cocatalyst for photocatalytic hydrogen production, *Appl. Surf. Sci.*, 2019, **487**, 734–742.
- 32 R. Qin, J. Nong, K. Wang, Y. Liu, S. Zhou, M. Hu and G. Shan, Recent advances in flexible pressure sensors based on MXene materials, *Adv. Mater.*, 2024, **36**(24), 2312761.
- 33 L. Han, W. Zeng, Y. Dong, X. Wang and L. Lin, Mapping and Simultaneous Detection of Arterial and Venous Pulses using Large-Scale High-Density Flexible Piezoelectret Sensor Array, *Adv. Electron. Mater.*, 2022, **8**(9), 2200012.
- 34 J. Chen, K. Sun, R. Zheng, Y. Sun, H. Yang, Y. Zhong and X. Li, Three-dimensional arterial pulse signal acquisition in time domain using flexible pressure-sensor dense arrays, *Micromachines*, 2021, **12**(5), 569.
- 35 Y. C. Huang, Y. H. Chang, S. M. Cheng, S. J. S. Lin, C. J. Lin and Y. C. Su, Applying pulse spectrum analysis to facilitate the diagnosis of coronary artery disease, *J. Evidence-Based Complementary Altern. Med.*, 2019, **2019**(1), 2709486.
- 36 J. Wang, G. Xia, L. Xia, Y. Chen, Q. Li, H. Zeng and Y. Chen, HCNT/AgNPs/PVA/PAM hydrogel-based flexible pressure sensor for physiological monitoring, *J. Mater. Sci.: Mater. Electron.*, 2024, **35**(29), 1931.
- 37 T. Zhao, J. Lv, B. Liu, H. Zhu and H. Zhang, A highly sensitive flexible pressure sensor based on laser-induced graphene and a composite dielectric structure, *Sens. Actuators, A*, 2023, **358**, 114460.
- 38 H. Guan, J. Meng, Z. Cheng and X. Wang, Processing natural wood into a high-performance flexible pressure sensor, *ACS Appl. Mater. Interfaces*, 2020, **12**(41), 46357–46365.
- 39 K. Cao, M. Wu, J. Bai, Z. Wen, J. Zhang, T. Wang and L. Jiang, Beyond skin pressure sensing: 3D printed laminated graphene pressure sensing material combines extremely low detection limits with wide detection range, *Adv. Funct. Mater.*, 2022, **32**(28), 2202360.
- 40 M. Yang, Y. Cheng, Y. Yue, Y. Chen, H. Gao, L. Li and Y. Gao, High-performance flexible pressure sensor with a self-healing function for tactile feedback, *Adv. Sci.*, 2022, **9**(20), 2200507.
- 41 F. Huang, G. Hu, Z. Yu, Y. Pan, H. Yao, C. Tang and H. Zhang, Highly sensitive and wide linearity flexible pressure sensor with randomly distributed columnar arrays, *J. Mater. Sci.*, 2023, **58**(8), 3735–3751.
- 42 Y. Li, Y. Cui, M. Zhang, X. Li, R. Li, W. Si and C. Huang, Ultrasensitive pressure sensor sponge using liquid metal modulated nitrogen-doped graphene nanosheets, *Nano Lett.*, 2022, **22**(7), 2817–2825.
- 43 Q. Yue, S. Xiao, Z. Li, J. Yang, B. Chen, J. Feng and T. Wang, Ultra-sensitive pressure sensors based on large alveolar deep tooth electrode structures with greatly stretchable oriented fiber membrane, *Chem. Eng. J.*, 2022, **443**, 136370.
- 44 Y. Lv, L. Min, F. Niu, X. Chen, B. Zhao, Y. Liu and K. Pan, Wrinkle-structured MXene film assists flexible pressure sensors with superhigh sensitivity and ultrawide detection range, *Nanocomposites*, 2022, **8**(1), 81–94.

